

VessShape: Few-shot 2D blood vessel segmentation by leveraging shape priors from synthetic images

Wesley Nogueira Galvão¹ and Cesar H. Comin^{1,*}

¹*Department of Computer Science, Federal University of São Carlos, São Carlos, SP, Brazil*

(Dated: September 28, 2025)

Semantic segmentation of blood vessels is a crucial task in medical image analysis, but its progress is often hindered by the scarcity of large annotated datasets and the poor generalization of models across different imaging modalities. A key aspect is the tendency of Convolutional Neural Networks (CNNs) to learn texture-based features, which limits their performance when applied to new domains with different visual characteristics. We hypothesize that leveraging the universal geometric prior of vessel-like shapes, tubular and branching structures, can lead to more robust and data-efficient models. To investigate this, we introduce VessShape, a large-scale 2D synthetic dataset designed to instill a shape bias in segmentation models. VessShape consists of images with procedurally generated tubular geometries combined with a wide variety of foreground and background textures, encouraging models to learn shape cues rather than textures. We demonstrate that a model pretrained on VessShape achieves strong few-shot segmentation performance on two real-world datasets from different domains, requiring only four to ten samples for fine-tuning. Furthermore, the model exhibits notable zero-shot capabilities, effectively segmenting vessels in unseen domains without any target-specific training. Our results indicate that pretraining with a strong shape bias can be an effective strategy to overcome data scarcity and improve model generalization in blood vessel segmentation.

Keywords: Blood vessel segmentation, shape bias, domain adaptation, few-shot learning

I. INTRODUCTION

The semantic segmentation of blood vessels is an active area of research, driven by the demand for precise and automated analysis of medical images in both human and animal tissues. A significant challenge in this task is the labor-intensive process of manual annotation, which requires domain expertise to create accurate segmentation masks.

This annotation bottleneck has led to a scarcity of large-scale datasets, which limits the training capacity of deep learning models. For instance, widely used public datasets such as DRIVE [1] and CHASE_DB1 [2] contain only a few dozen annotated images each. Although recent efforts have introduced new datasets [3, 4], the availability of large and diverse collections remains limited. This problem is compounded by significant domain shifts between different imaging modalities, such as retinal fundus photography and cerebral cortex microscopy. Variations in texture, vessel density, and caliber hinder the ability of models trained in one domain to generalize to another.

Transfer learning is a common strategy to address these limitations. By reusing representations learned on a source domain, models can achieve better performance on a target domain, even with limited data. Techniques such as fine-tuning and domain adaptation allow models pretrained on large-scale natural image datasets, like ImageNet [5], to be adapted for biomedical segmentation tasks [6].

However, a potential pitfall of standard transfer learning is the inherent bias of Convolutional Neural Networks (CNNs) toward learning texture-based features rather

than geometric shapes [7, 8]. This texture bias can limit generalization across domains with different visual styles. Research has shown that models trained with an emphasis on shape cues exhibit improved performance and robustness [7]. This suggests that transferring shape representations, rather than texture-rich features, could be a more effective strategy for few-shot blood vessel segmentation.

The task of blood vessel segmentation is particularly well suited for a shape-centric approach. The fundamental geometry of blood vessels, tubular and branching structures, is a consistent prior across diverse imaging modalities, from retinal fundus photographs to cerebral cortex microscopy images. While textures and other visual characteristics may vary significantly between these domains, the underlying shape remains a universal identifier. For example, a human observer who has learned to identify vessels in one modality can readily recognize them in another, as illustrated in Figure 1.

Based on this observation, we hypothesize that a model pretrained on a source domain with a strong shape bias will require only a few annotated samples to adapt to a new target domain. We expect such a model to outperform one trained from scratch in the target domain by effectively reusing its learned geometric priors. To test this hypothesis, we introduce VessShape, a large-scale synthetic dataset designed for pretraining shape-aware segmentation models. VessShape consists of 2D images with tubular, vessel-like structures paired with a wide variety of foreground and background textures. By fixing the geometric priors while diversifying the textures, the dataset explicitly encourages models to learn robust shape features over superficial texture cues.

In this work, we demonstrate that a model pretrained on VessShape achieves strong few-shot performance, accu-

* Corresponding author: comin@ufscar.br

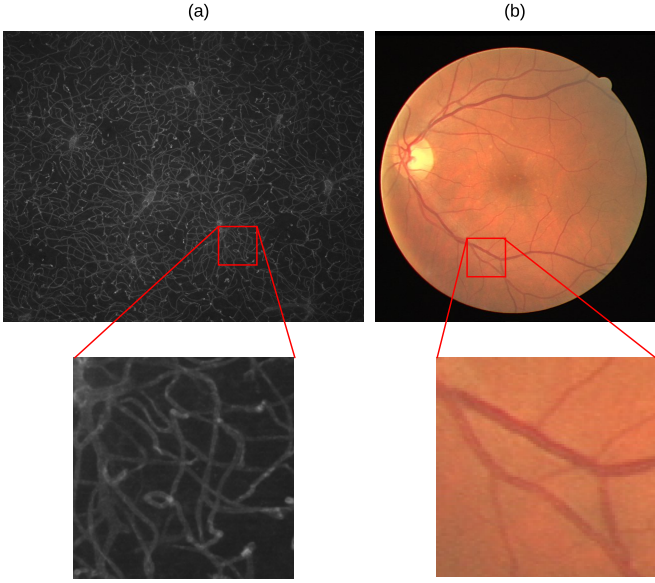


FIG. 1. Illustration of the universality of vessel shape. (a) Fluorescence microscopy sample of a mouse cortex. (b) Fundus photograph of a human eye. Despite having different textures, the vessels have similar shapes.

rately segmenting vasculature in different target domains using only four to ten annotated samples for fine-tuning. Furthermore, we observe remarkable zero-shot capabilities, where the pretrained model can effectively segment vessels in new domains without any target-specific training.

II. RELATED WORKS

Many previous work has considered shape priors for medical image segmentation. This is possible when organelles, cells, or organs have a known shape and the segmentation process can assume an optimal shape or additional optimization criteria such as the requirement of smooth borders. Instance segmentation is probably the most common task in which shape priors have been explored. A particular challenge with blood vessel identification is that it usually requires a semantic segmentation of the image.

Before the popularity of deep learning methods, local shape priors were the dominant approach to vessel segmentation. Blood vessels tend to have a tubular structure. Thus, the usual approach was to develop filters aimed at identifying tubular objects. A popular line of research was based on the eigenvalues of the Hessian matrix [9, 10]. Arguably, the most popular Hessian-based method is the Frangi filter [11], which consists of combining the eigenvalues to define a tubularity score for the pixels of the vessels. Another popular line of research was based on the definition of line or Gabor filter templates to identify relevant vessel structures. An important drawback of these methods is that the tubularity assumption is not valid at bifurcation and termination points.

With the emergence of deep learning, some works have explored adding shape priors during network training [12]. Priors have been added on the network input using vesselness filters [13–15], on the network architecture using learnable vesselness or Gabor filters [16–18] and on the network output using topology-aware loss functions [19–21]. For neural networks, it is simpler and likely more flexible to consider a data-based approach to add shape priors to the model. That is, to focus on generating a large and diverse set of images containing a priori knowledge regarding the structure of blood vessels. To our knowledge, no previous work tried to use the same method considered in our work. The closest approach is to generate synthetic images that are as similar as possible to the samples in the dataset. This has been done using two main strategies: i) using an appearance model of the vessels and image background [22–25] and ii) using style transfer or a generative model to create the samples.

Modeling-based approaches usually start by generating a biologically plausible topology of the vasculature, followed by the definition of varying radii for vessel segments and the inclusion of texture for the vessels and the background. The typical noise found in the imaging modality of interest is also modeled. An important recent work in this direction is a foundation model called VesselFM [23] that was trained on a large number of synthetic and real images.

Regarding generative models, most works in the literature use inductive learning, applying Generative Adversarial Networks (GANs) to create samples [26–29]. Synthetic samples conform to the learned patterns from the real dataset, allowing the generation of realistic images. Recent works considered diffusion models for the same task [30–32]. Some studies also developed style transfer approaches for domain adaptation between different datasets [33–35].

The main drawback of the aforementioned works is that the network is trained to reproduce the shape and texture of blood vessels in specific datasets. Changes in the texture of the vessels due to diseases or modifications in the imaging device can lead to low segmentation performance. In addition, models must be trained for specific imaging modalities, even if annotated data are scarce. Our approach aims at training neural networks to segment any vascular tissue that follows the shape priors acquired from VessShape.

III. METHODOLOGY

A. The VessShape Dataset

VessShape¹ defines the geometry of its synthetic images using Bézier curves, which allow a flexible and controlled

¹ Dataset repository: <https://github.com/galvaowesley/vess-shape-dataset>

representation of tubular shapes. Each vascular segment is described by an n th-order Bézier curve with control points $\{\mathbf{p}_i\}_{i=0}^n$. Segment tortuosity is adjusted by small perturbations to these control points, ensuring realistic and diverse vessel geometry. The Bézier curve $\mathbf{c}(t)$ of a vessel segment is given by Equation 1, where t varies from 0 to 1.

$$\mathbf{c}(t) = \sum_{i=0}^n \binom{n}{i} (1-t)^{n-i} t^i \mathbf{p}_i, \quad (1)$$

To generate a curve, the first (\mathbf{p}_0) and last (\mathbf{p}_n) control points are randomly drawn with uniform probability. The remaining control points are generated by defining $n - 2$ equally spaced points between a line connecting \mathbf{p}_0 and \mathbf{p}_1 . Each of these points is then displaced by a random amount along a normal vector \mathbf{n}_l . This normal vector is a unit vector perpendicular to the line between \mathbf{p}_0 and \mathbf{p}_1 . The displacement amount is drawn from a uniform distribution in $[-\delta, \delta]$. Lower values of δ lead to more straight curves.

For the generation of the binary mask M , each curve is discretized by sampling points at a sufficient resolution to capture its curvature, which are then sequentially connected to form a 1-pixel-thick polyline on the image grid. Subsequently, a binary morphological dilation with a disk-shaped structuring element of radius r_0 is applied, assigning a constant tubular thickness to the segments.

To generate each binary mask, the number of segments K , the order n of the Bézier curves, the displacement scale δ and the radius r_0 are all randomly sampled from an interval to ensure a wide variety of shapes. Table I summarizes the parameters used in the VessShape dataset generation, along with their sampling ranges and descriptions.

To compose the final image I from a binary mask M , a foreground texture F and a background texture B are inserted into, respectively, the generated vessel segments and the background of the image. The textures are randomly selected from the ImageNet validation set [5]. Specifically, for each mask M , two images are randomly drawn from two distinct classes of the ImageNet dataset. The images are then randomly cropped and resized to the target dimensions ($H \times W$). An alpha matte A is then generated by smoothing M with a Gaussian filter of standard deviation σ and normalizing its values to the $[0, 1]$ range. The textures are subsequently blended using this matte according to Equation 2,

$$I = A F + (1 - A) B, \quad (2)$$

which ensures that vessel regions ($A \approx 1$) preserve the foreground while non-vessel regions ($A \approx 0$) retain the background.

Parameter σ controls the smoothness of the vessel boundaries. Examples of generated masks and images are shown in Figure 2.

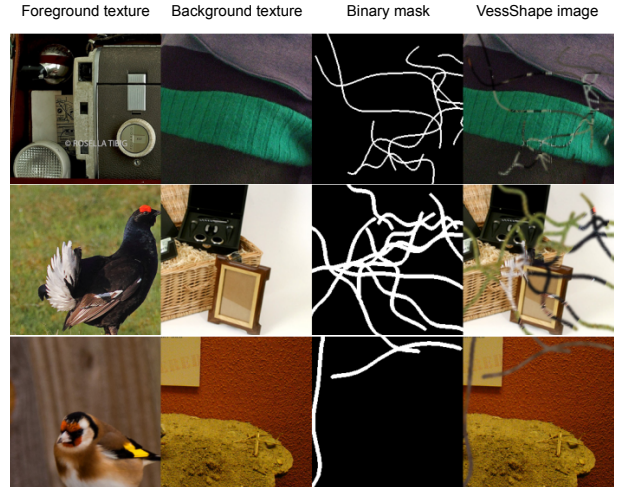


FIG. 2. Examples of ImageNet samples, synthetic geometry and respective VessShape images. The ImageNet samples are used as textures for the synthetic binary masks, defining the respective VessShape image.

B. Real-world data for validation

To quantify the usefulness of the shape bias introduced by the VessShape dataset, we consider two blood vessel datasets: DRIVE and VessMAP. The DRIVE dataset [1] serves as a popular standard for benchmarking retinal vessel segmentation algorithms and is composed of 40 fundus photographs split into 20 for training and 20 for testing, each measuring 584×565 pixels. The VessMAP dataset [36] consists of 100 images, 256×256 pixels each, acquired via fluorescence microscopy of the mouse cortex. It was curated to include a variety of challenging vascular features, such as inconsistent noise and contrast levels, different vessel sizes, prominent imaging artifacts, and intensity fluctuations within vessel structures.

The two datasets originate from fundamentally different imaging modalities, resulting in distinct characteristics. The fundus images in DRIVE, which capture the entire retina, possess a clear global structure that includes landmarks like the optic disk. The samples also contain many very thin vessels which are challenging to segment. In contrast, the VessMAP images are highly magnified views of small cortical areas and have no discernible global organization. The borders of the vessels are generally less defined than the vessels from DRIVE. Another key difference is that, without any processing, the vessels in VessMAP are bright with dark backgrounds while the vessels in DRIVE are dark with bright backgrounds. Figure 3 shows one sample from each dataset.

TABLE I. Main parameters used for generating the VessShape dataset.

Parameter	Range	Description
Number of curves K	[1, 20]	Number of branches/vessels generated per sample.
Control points $n+1$	[2, 20]	Bézier curve complexity (order n).
Displacement scale δ (px)	[50.0, 150.0]	Controls curvature/tortuosity via the typical amplitude of control-point displacement.
Initial radius r_0 (px)	[1, 5]	Basal vessel thickness; a smooth taper is applied along the branch.
Matting blur σ	[1, 2]	Standard deviation of the Gaussian used for $A = G_\sigma * M$.

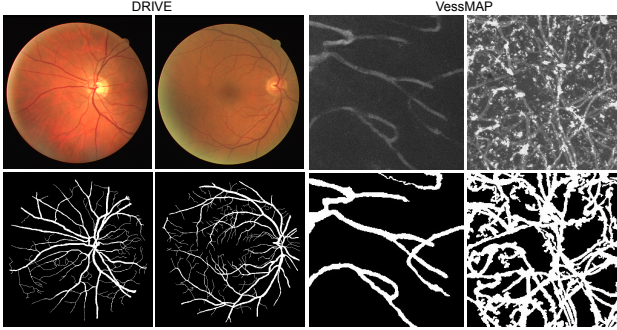


FIG. 3. Samples from the DRIVE and VessMAP datasets and their respective ground-truth masks.

C. Model architectures and training strategies

We adopt an encoder-decoder U-Net design, that is, the decoder is symmetrical to the encoder and the model contains skip connections between different encoder-decoder stages. Two models are compared, one with a ResNet18 and the other with a ResNet50 encoder [37]. The models were instantiated from the *Segmentation Models Pytorch* Python package².

Two training scenarios are considered. In the first, training is done from scratch separately on the DRIVE and VessMAP datasets to establish a baseline. The second scenario consists of pretraining on the VessShape dataset and fine-tuning on DRIVE and VessMAP to measure the transferability and sample efficiency of the learned representations. These two scenarios involve three distinct training procedures: i) pretraining on VessShape, ii) fine-tuning on real-world data and iii) training from scratch on real-world data. These procedures are described next.

D. Pretraining on VessShape

The pretraining on VessShape aims to expose the model to a wide variety of tubular geometries while keeping texture as a secondary cue, which tends to benefit the segmentation of thin structures. Each training sample is generated on-the-fly, and we apply channel-wise normalization with ImageNet statistics. This continual reshuffling

TABLE II. Pretraining hyperparameters on VessShape.

Hyperparameter	VSUNet50	VSUNet18
Batch size	96	192
Learning rate	1.0e-3	1.0e-2
Learning rate decay	0.0	0.0
Weight decay	1.0e-4	0.0

TABLE III. Performance of VSUNet variants after pretraining on VessShape.

Metric	VSUNet50	VSUNet18
Dice	0.861 ± 0.022	0.859 ± 0.077
Acc	0.960 ± 0.008	0.956 ± 0.037
IoU	0.758 ± 0.032	0.761 ± 0.096
Prec	0.780 ± 0.037	0.774 ± 0.096
Rec	0.964 ± 0.012	0.974 ± 0.018

of appearance paired with stable geometric rules injects a strong shape bias while discouraging memorization of superficial textures. The model is optimized to minimize the average loss over this effectively unbound synthetic stream.

We pre-train two U-Net models with ResNet18 and ResNet50 encoders, referred to as VSUNet18 and VSUNet50. VSUNet18 was exposed to about 7.1 million synthetic images in roughly 8.6 hours of training, and VSUNet50 to about 53.0 million in roughly 78.3 hours. Table II lists the hyperparameters, and Table III summarizes training performance on VessShape. All pretraining runs were executed on a workstation with 24 logical CPU cores and a single NVIDIA GeForce RTX 3090 GPU.

E. Fine-tuning

- Datasets (VessMAP e DRIVE)

- Procedure

² https://github.com/qubvel/segmentation_models.pytorch

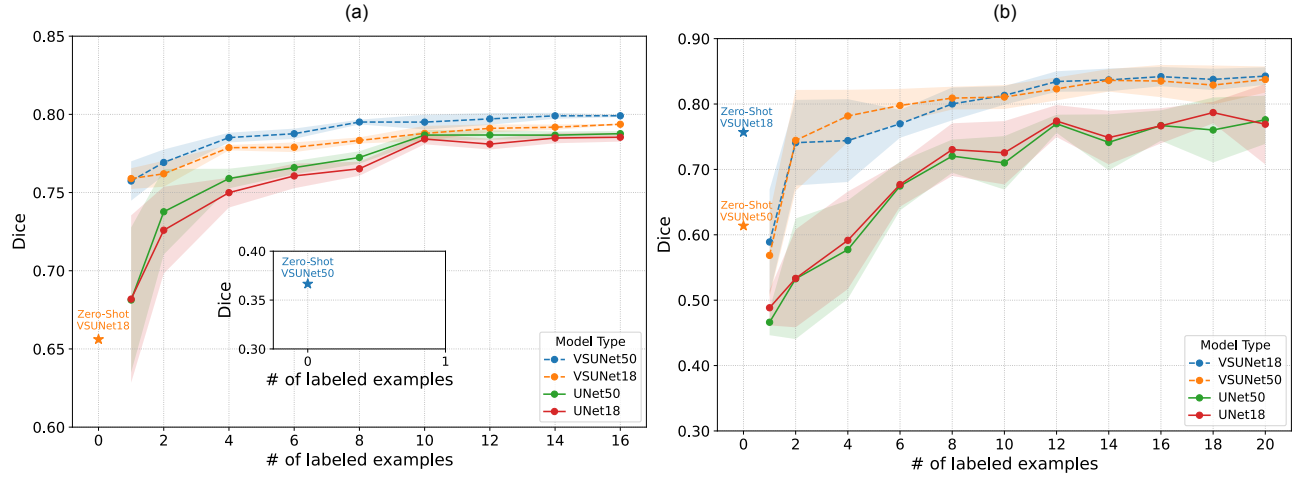


FIG. 4. ??.

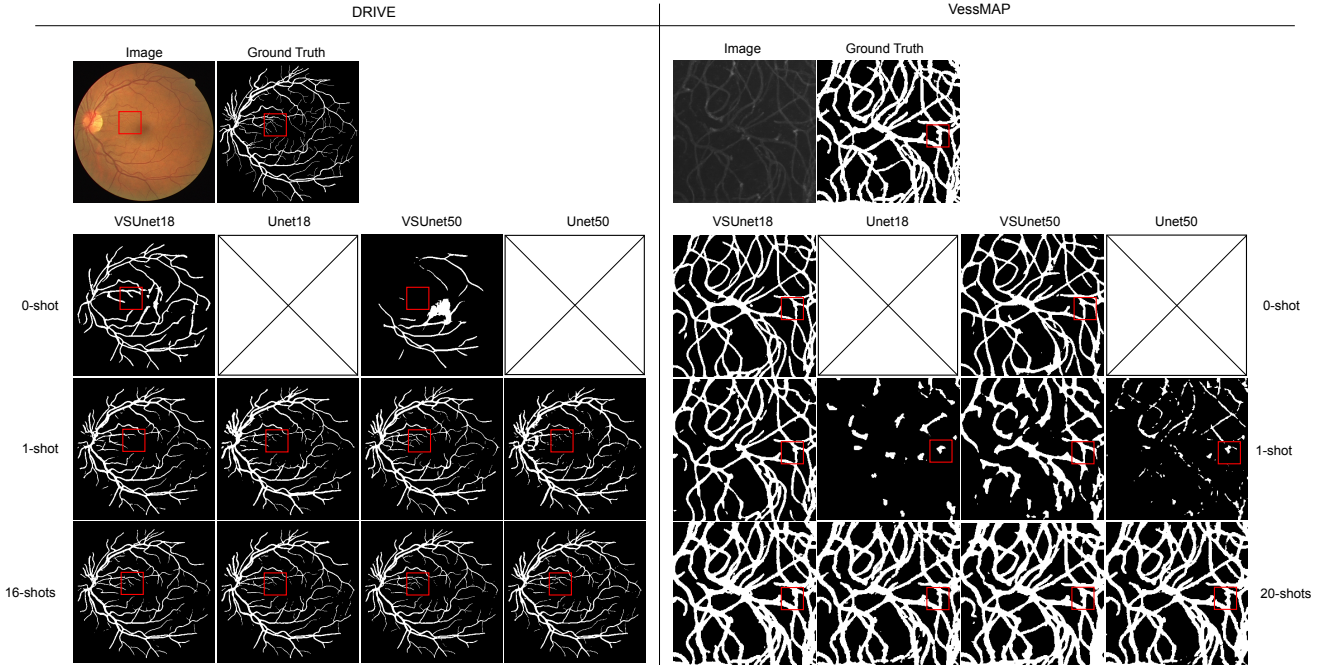


FIG. 5. ??.

F. Training from scratch on natural datasets

IV. RESULTS

V. CONCLUSION

We proposed a strategy centered on instilling a strong shape bias in deep learning models by pretraining them on VessShape, a large-scale synthetic dataset. By combining simple, universal vessel-like geometries with highly diverse textures, VessShape encourages models to learn robust shape priors instead of domain-specific texture features.

Our experiments demonstrated the effectiveness of this approach. A model pretrained on VessShape achieved strong few-shot performance on two distinct and challenging real-world datasets, DRIVE (retinal fundus photography) and VessMAP (cerebral cortex microscopy), requiring only a handful of annotated samples to adapt to these new domains. Furthermore, the model exhibited remarkable zero-shot capabilities, successfully identifying vessel structures without any fine-tuning. These results confirm our hypothesis that the use of a fundamental geometric prior is a powerful method to improve data efficiency and model robustness against domain shifts.

TABLE IV. Few-shot and zero-shot segmentation on VessMAP and DRIVE. Values are mean \pm standard deviation over repeated runs (fine-tuning for VSUNet models and training from scratch for U-Net baselines) evaluated on each dataset test set. Zero-shot rows come from a single pretrained inference (no deviation available).

Dataset	#Examples	Model	Dice	Acc	IoU	Prec	Rec
DRIVE	0	VSUNet18	0.656 \pm 0.000	0.907 \pm 0.000	0.490 \pm 0.000	0.629 \pm 0.000	0.699 \pm 0.000
		VSUNet50	0.367 \pm 0.000	0.888 \pm 0.000	0.230 \pm 0.000	0.728 \pm 0.000	0.275 \pm 0.000
	1	VSUNet18	0.759 \pm 0.007	0.941 \pm 0.002	0.612 \pm 0.009	0.787 \pm 0.021	0.741 \pm 0.019
		VSUNet50	0.757 \pm 0.013	0.939 \pm 0.006	0.611 \pm 0.016	0.773 \pm 0.046	0.754 \pm 0.039
		UNet18	0.682 \pm 0.054	0.919 \pm 0.016	0.523 \pm 0.058	0.717 \pm 0.079	0.690 \pm 0.118
		UNet50	0.681 \pm 0.046	0.916 \pm 0.031	0.523 \pm 0.050	0.722 \pm 0.099	0.690 \pm 0.110
		VSUNet18	0.794 \pm 0.000	0.950 \pm 0.000	0.658 \pm 0.000	0.833 \pm 0.004	0.762 \pm 0.003
	16	VSUNet50	0.799 \pm 0.001	0.952 \pm 0.000	0.666 \pm 0.001	0.846 \pm 0.003	0.762 \pm 0.004
		UNet18	0.785 \pm 0.003	0.946 \pm 0.001	0.647 \pm 0.004	0.795 \pm 0.005	0.781 \pm 0.004
		UNet50	0.788 \pm 0.002	0.947 \pm 0.001	0.650 \pm 0.002	0.807 \pm 0.006	0.774 \pm 0.004
		VSUNet18	0.757 \pm 0.000	0.886 \pm 0.000	0.616 \pm 0.000	0.846 \pm 0.000	0.696 \pm 0.000
VessMAP	0	VSUNet50	0.614 \pm 0.000	0.817 \pm 0.000	0.472 \pm 0.000	0.746 \pm 0.000	0.605 \pm 0.000
		VSUNet18	0.589 \pm 0.080	0.705 \pm 0.205	0.455 \pm 0.088	0.675 \pm 0.205	0.738 \pm 0.148
	1	VSUNet50	0.569 \pm 0.063	0.708 \pm 0.203	0.439 \pm 0.071	0.683 \pm 0.208	0.700 \pm 0.167
		UNet18	0.488 \pm 0.027	0.674 \pm 0.184	0.362 \pm 0.032	0.682 \pm 0.204	0.622 \pm 0.210
		UNet50	0.466 \pm 0.020	0.665 \pm 0.181	0.343 \pm 0.025	0.674 \pm 0.206	0.604 \pm 0.215
		VSUNet18	0.843 \pm 0.013	0.901 \pm 0.021	0.739 \pm 0.018	0.825 \pm 0.049	0.888 \pm 0.048
	20	VSUNet50	0.837 \pm 0.020	0.905 \pm 0.025	0.732 \pm 0.026	0.851 \pm 0.032	0.850 \pm 0.027
		UNet18	0.769 \pm 0.062	0.880 \pm 0.034	0.645 \pm 0.075	0.864 \pm 0.045	0.737 \pm 0.094
		UNet50	0.776 \pm 0.037	0.880 \pm 0.035	0.653 \pm 0.046	0.855 \pm 0.041	0.752 \pm 0.051

Although our method shows significant promise, there are avenues for future work. The current geometry generation in VessShape, based on Bézier curves, could be extended to include more complex and biologically plausible vascular topologies, such as true bifurcations and network-like structures. Furthermore, extending the VessShape generation framework to 3D would allow this pretraining strategy to be applied to volumetric medical imaging modalities such as CT and MRI. Future studies could also explore the application of a shape-centric pretraining approach to the segmentation of other tubular structures in biology, such as neurons or airways.

Our work underscores a valuable principle: for seg-

mentation tasks with strong and consistent shape priors, abstracting away from realism to focus on core geometric features can be a more effective and generalizable pre-training strategy than attempting to perfectly mimic the appearance of a single target domain.

FUNDING

C. H. Comin thanks FAPESP (grant no. 21/12354-8) for financial support.

-
- [1] Joes Staal, Michael D. Abràmoff, Meindert Niemeijer, Max A. Viergever, and Bram Van Ginneken, “Ridge-based vessel segmentation in color images of the retina,” *IEEE Transactions on Medical Imaging* **23**, 501–509 (2004).
- [2] Muhammad Moazam Fraz, Paolo Remagnino, Andreas Hoppe, Bunyarit Uyyanonvara, Alicja R. Rudnicka, Christopher G. Owen, and Sarah A. Barman, “An ensemble classification-based approach applied to retinal blood vessel segmentation,” *IEEE Transactions on Biomedical Engineering* **59**, 2538–2548 (2012).
- [3] Kai Jin, Xingru Huang, Jingxing Zhou, Yunxiang Li, Yan Yan, Yibao Sun, Qianni Zhang, Yaqi Wang, and Juan Ye, “Fives: A fundus image dataset for artificial intelligence based vessel segmentation,” *Scientific data* **9**, 475 (2022).
- [4] Jonathan Fhima, Jan Van Eijgen, Marie-Isaline Billen Moulin-Romsée, Hélène Brackenier, Hana Kulenovic, Valérie Debeuf, Marie Vangilbergen, Moti Freiman, Ingeborg Stalmans, and Joachim A Behar, “Lunet: deep learning for the segmentation of arterioles and venules in high resolution fundus images,” *Physiological Measurement* **45**, 055002 (2024).
- [5] Jia Deng, Wei Dong, Richard Socher, Li-Jia Li, Kai Li, and Li Fei-Fei, “ImageNet: A large-scale hierarchical image database,” in *2009 IEEE Conference on Computer Vision and Pattern Recognition* (IEEE, 2009) pp. 248–255.
- [6] Riaan Zoetmulder, Efstratios Gavves, Matthan Caan, and Henk Marquering, “Domain- and task-specific transfer learning for medical segmentation tasks,” *Computer Methods and Programs in Biomedicine* **214**, 106539 (2022).

- [7] Robert Geirhos, Patricia Rubisch, Claudio Michaelis, Matthias Bethge, Felix A Wichmann, and Wieland Brendel, “Imagenet-trained CNNs are biased towards texture; increasing shape bias improves accuracy and robustness,” in *International Conference on Learning Representations* (2019).
- [8] Md Amirul Islam, Matthew Kowal, Patrick Esser, Sen Jia, Björn Ommer, Konstantinos G. Derpanis, and Neil Bruce, “Shape or texture: Understanding discriminative features in {cnn}s,” in *International Conference on Learning Representations* (2021).
- [9] Muhammad Moazam Fraz, Paolo Remagnino, Andreas Hoppe, Bunyarat Uyyanonvara, Alicja R Rudnicka, Christopher G Owen, and Sarah A Barman, “Blood vessel segmentation methodologies in retinal images—a survey,” *Computer methods and programs in biomedicine* **108**, 407–433 (2012).
- [10] Yoshinobu Sato, Shin Nakajima, Nobuyuki Shiraga, Hideki Atsumi, Shigeyuki Yoshida, Thomas Koller, Guido Gerig, and Ron Kikinis, “Three-dimensional multi-scale line filter for segmentation and visualization of curvilinear structures in medical images,” *Medical image analysis* **2**, 143–168 (1998).
- [11] Alejandro F Frangi, Wiro J Niessen, Koen L Vincken, and Max A Viergever, “Multiscale vessel enhancement filtering,” in *International conference on medical image computing and computer-assisted intervention* (Springer, 1998) pp. 130–137.
- [12] Simon Bohlender, Ilkay Oksuz, and Anirban Mukhopadhyay, “A survey on shape-constraint deep learning for medical image segmentation,” *IEEE Reviews in Biomedical Engineering* **16**, 225–240 (2021).
- [13] Abir Affane, Jonas Lamy, Marie-Ange Lebre, and Antoine Vacavant, “Robust deep 3-d architectures based on vascular patterns for liver vessel segmentation,” *Informatics in Medicine Unlocked* **34**, 101111 (2022).
- [14] Dewei Hu, Hao Li, Han Liu, and Ipek Oguz, “Domain generalization for retinal vessel segmentation via hessian-based vector field,” *Medical image analysis* **95**, 103164 (2024).
- [15] Guillaume Garret, Antoine Vacavant, and Carole Frindel, “Deep vessel segmentation based on a new combination of vesselness filters,” in *2024 IEEE International Symposium on Biomedical Imaging (ISBI)* (IEEE, 2024) pp. 1–5.
- [16] Cheng Chen, Kangneng Zhou, Siyu Qi, Tong Lu, and Ruoxiu Xiao, “A learnable gabor convolution kernel for vessel segmentation,” *Computers in Biology and Medicine* **158**, 106892 (2023).
- [17] Weilin Fu, Katharina Breininger, Roman Schaffert, Nishanth Ravikumar, Tobias Würfl, Jim Fujimoto, Eric Moult, and Andreas Maier, “Frangi-net,” in *Bildverarbeitung für die Medizin 2018: Algorithmen-Systeme-Anwendungen. Proceedings des Workshops vom 11. bis 13. März 2018 in Erlangen* (Springer, 2018) pp. 341–346.
- [18] Egor Volkov and Alexey Averkin, “Modification of u-net architecture based on gabor filters with trainable parameters to improve biomarker segmentation on oct images,” in *2025 VI International Conference on Neural Networks and Neurotechnologies (NeuroNT)* (IEEE, 2025) pp. 66–68.
- [19] Suprosanna Shit, Johannes C Paetzold, Anjany Sekuboyina, Ivan Ezhov, Alexander Unger, Andrey Zhylka, Josien PW Pluim, Ulrich Bauer, and Bjoern H Menze, “cldice-a novel topology-preserving loss function for tubular structure segmentation,” in *Proceedings of the IEEE/CVF conference on computer vision and pattern recognition* (2021) pp. 16560–16569.
- [20] Xiaoling Hu, Fuxin Li, Dimitris Samaras, and Chao Chen, “Topology-preserving deep image segmentation,” *Advances in neural information processing systems* **32** (2019).
- [21] Alexander H Berger, Laurin Lux, Nico Stucki, Vincent Bürgin, Suprosanna Shit, Anna Banaszak, Daniel Rueckert, Ulrich Bauer, and Johannes C Paetzold, “Topologically faithful multi-class segmentation in medical images,” in *International Conference on Medical Image Computing and Computer-Assisted Intervention* (Springer, 2024) pp. 721–731.
- [22] Giles Tetteh, Velizar Efremov, Nils D Forkert, Matthias Schneider, Jan Kirschke, Bruno Weber, Claus Zimmer, Marie Piraud, and Björn H Menze, “Deepvesselnet: Vessel segmentation, centerline prediction, and bifurcation detection in 3-d angiographic volumes,” *Frontiers in Neuroscience* **14**, 592352 (2020).
- [23] Bastian Wittmann, Yannick Wattenberg, Tamaz Amiranashvili, Suprosanna Shit, and Bjoern Menze, “veselfm: A foundation model for universal 3d blood vessel segmentation,” in *Proceedings of the Computer Vision and Pattern Recognition Conference* (2025) pp. 20874–20884.
- [24] Bastian Wittmann, Lukas Glandorf, Johannes C Paetzold, Tamaz Amiranashvili, Thomas Wälchli, Daniel Razansky, and Bjoern Menze, “Simulation-based segmentation of blood vessels in cerebral 3d octa images,” in *International Conference on Medical Image Computing and Computer-Assisted Intervention* (Springer, 2024) pp. 645–655.
- [25] Joël Mathys, Andreas Plesner, Jorel Elmiger, and Roger Wattenhofer, “Synthetic data for blood vessel network extraction,” in *Will Synthetic Data Finally Solve the Data Access Problem?* (2025).
- [26] Aram You, Jin Kuk Kim, Ik Hee Ryu, and Tae Keun Yoo, “Application of generative adversarial networks (gan) for ophthalmology image domains: a survey,” *Eye and Vision* **9**, 6 (2022).
- [27] Paolo Andreini, Giorgio Ciano, Simone Bonechi, Caterina Graziani, Veronica Lachi, Alessandro Mecocci, Andrea Sodi, Franco Scarselli, and Monica Bianchini, “A two-stage gan for high-resolution retinal image generation and segmentation,” *Electronics* **11**, 60 (2021).
- [28] Alireza Tavakkoli, Sharif Amit Kamran, Khondker Fariha Hossain, and Stewart Lee Zuckerbrod, “A novel deep learning conditional generative adversarial network for producing angiography images from retinal fundus photographs,” *Scientific Reports* **10**, 21580 (2020).
- [29] Pedro Costa, Adrian Galdran, Maria Ines Meyer, Meindert Niemeijer, Michael Abràmoff, Ana Maria Mendonça, and Aurélio Campilho, “End-to-end adversarial retinal image synthesis,” *IEEE transactions on medical imaging* **37**, 781–791 (2017).
- [30] Sojung Go, Younghoon Ji, Sang Jun Park, and Soochahn Lee, “Generation of structurally realistic retinal fundus images with diffusion models,” in *Proceedings of the IEEE/CVF conference on computer vision and pattern recognition* (2024) pp. 2335–2344.
- [31] Zhanqiang Guo, Zimeng Tan, Jianjiang Feng, and Jie Zhou, “Vesseldiffusion: 3d vascular structure generation based on diffusion model,” *IEEE Transactions on Medical Imaging* (2025).
- [32] Zhifeng Wang, Renjiao Yi, Xin Wen, Chenyang Zhu, and Kai Xu, “Vastsd: Learning 3d vascular tree-state space

- diffusion model for angiography synthesis,” in *Proceedings of the Computer Vision and Pattern Recognition Conference* (2025) pp. 15693–15702.
- [33] Linkai Peng, Li Lin, Pujin Cheng, Ziqi Huang, and Xiaoying Tang, “Unsupervised domain adaptation for cross-modality retinal vessel segmentation via disentangling representation style transfer and collaborative consistency learning,” in *2022 IEEE 19th International Symposium on Biomedical Imaging (ISBI)* (IEEE, 2022) pp. 1–5.
- [34] Shuo Chen, Da Ma, Sieun Lee, Timothy TL Yu, Gavin Xu, Donghuan Lu, Karteek Popuri, Myeong Jin Ju, Marinko V Sarunic, and Mirza Faisal Beg, “Segmentation-guided domain adaptation and data harmonization of multi-device retinal optical coherence tomography using cycle-consistent generative adversarial networks,” *Computers in Biology and Medicine* **159**, 106595 (2023).
- [35] Heping Chen, Yan Shi, Bin Bo, Denghui Zhao, Peng Miao, Shanbao Tong, and Chunliang Wang, “Real-time cerebral vessel segmentation in laser speckle contrast image based on unsupervised domain adaptation,” *Frontiers in Neuroscience* **15**, 755198 (2021).
- [36] Matheus Viana da Silva, Natália de Carvalho Santos, Julie Ouellette, Baptiste Lacoste, and Cesar H Comin, “A new dataset for measuring the performance of blood vessel segmentation methods under distribution shifts,” *Plos one* **20**, e0322048 (2025).
- [37] Kaiming He, Xiangyu Zhang, Shaoqing Ren, and Jian Sun, “Deep residual learning for image recognition,” in *Proceedings of the IEEE conference on computer vision and pattern recognition* (2016) pp. 770–778.